

## Supplement Information

### One-Step Plasma-Enabled Catalytic Carbon Dioxide Hydrogenation to Higher Hydrocarbons: Significance of Catalyst-Bed Configuration

Jiajie Wang<sup>1,6</sup>, Mohammad S. AlQahtani<sup>1,2</sup>, Xiaoxing Wang<sup>1\*</sup>, Sean D. Knecht<sup>3</sup>, Sven G. Bilén<sup>3,4</sup>, Chunshan Song<sup>1,2,5\*</sup> and Wei Chu<sup>6</sup>

<sup>1</sup> Clean Fuels & Catalysis Program, EMS Energy Institute, Department of Energy and Mineral Engineering, The Pennsylvania State University, University Park, PA, 16802, USA

<sup>2</sup> Department of Chemical Engineering, The Pennsylvania State University, University Park, PA, 16802, USA

<sup>3</sup> School of Engineering Design, Technology, and Professional Programs, The Pennsylvania State University, University Park, PA, 16802, USA

<sup>4</sup> School of Electrical Engineering and Computer Science, The Pennsylvania State University, University Park, PA, 16802, USA

<sup>5</sup> Department of Chemistry, Faculty of Science, The Chinese University of Hong Kong, Shatin, NT, Hong Kong, China

<sup>6</sup> Department of Chemical Engineering, Sichuan University, Sichuan, P.R. China,

\*Email: [xuw4@psu.edu](mailto:xuw4@psu.edu); [cxs23@psu.edu](mailto:cxs23@psu.edu); [chunshansong@cuhk.edu.hk](mailto:chunshansong@cuhk.edu.hk)

## 1. Experiment

### 1.1 Catalyst preparation

The alumina-supported Co catalyst used in this study was prepared by a pore-filling incipient wetness impregnation using an aqueous solution containing  $\text{Co}(\text{NO}_3)_2 \cdot 6\text{H}_2\text{O}$  (Aldrich, > 98%). The support is  $\gamma\text{-Al}_2\text{O}_3$  (Sasol PURALOX TH 100/150) with specific surface area of 139  $\text{m}^2/\text{g}$ , the average pore diameter of 2.4 nm and the pore volume of 1.04  $\text{cm}^3/\text{g}$ . Prior to catalyst synthesis, the support was calcined in air at 550 °C for 2 hours at a ramp rate of 2 °C/min. The solution volume was 90% of the total pore volume of the carrier and was added dropwise to the support. The mixture was then dried in a vacuum oven at 60 °C overnight, followed by calcination in air at 400 °C for 2 hours at a ramp rate of 2 °C/min in a muffle furnace. The obtained catalyst sample was crushed and sieved to 18-35 mesh. The content of Co metal in the catalyst is 15 wt% (based on the support), which is referred to as 15Co in this paper.

## 1.2 Fixed-bed DBD plasma reactor

The plasma reaction was carried out in a packed-bed DBD reactor shown in Fig. S1. The reactor consists of a pair of quartz tubes, inner tube (6 mm O.D. × 4 mm I.D.) and outer tube (12 mm O.D. × 10 mm I.D.). The reactant gases are controlled by mass flow meters. The plasma was generated by a PVM500 AC power supply. The high-voltage electrode is a tungsten rod placed inside the inner quartz tube, and the ground electrode is an aluminum foil wrapped outside the outer quartz tube. The discharge gap is approximately 2 mm across and 50 mm in length. The applied plasma power is calculated by the Lissajous method based on the integral of the voltage signal recorded by the digital oscilloscope (Tektronix, TBS 1052B). Throughout the experiment, the discharge frequency of the plasma was fixed at 23.5 kHz, the input voltage was 14 ~ 20 kV, and the corresponding plasma power was 3.8~10.1 W. External capacitor value is 10 nF.

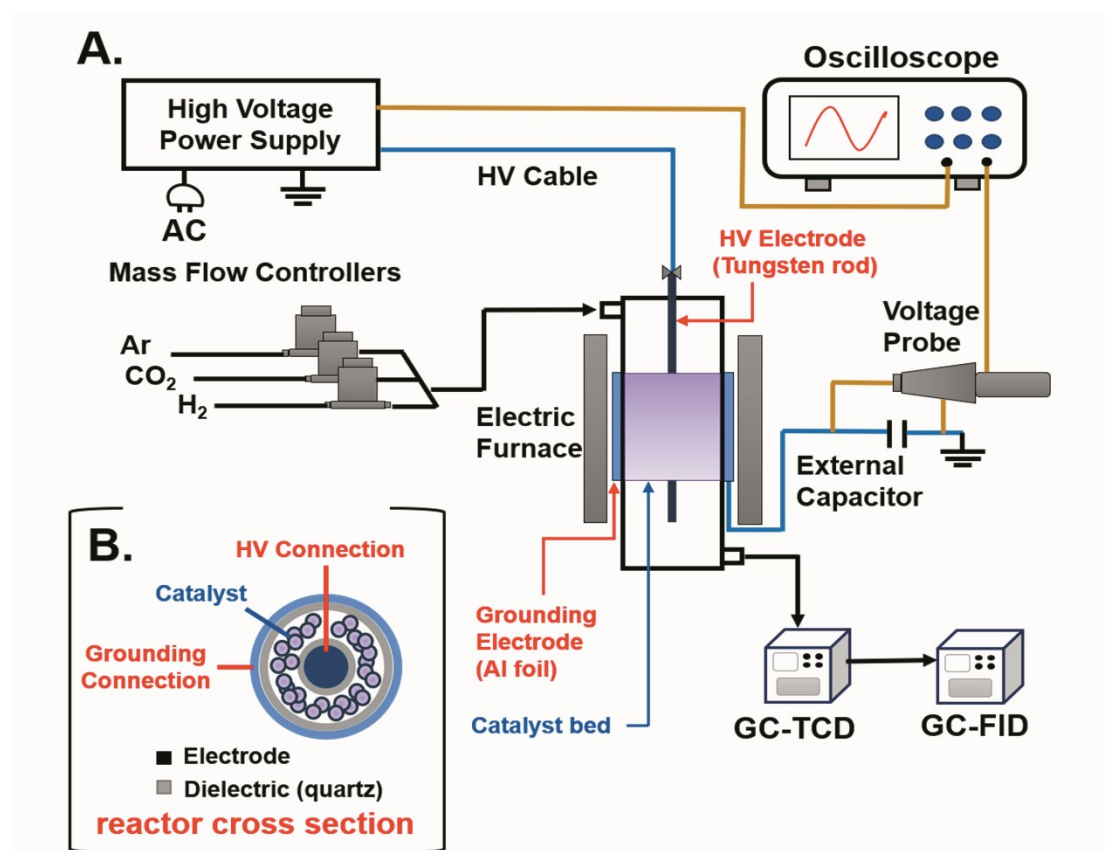


**Fig. S1.** Schematic diagram of A) plasma-catalysis experimental setup; and B) reactor cross section.

Before reaction, the catalyst was reduced in a pure hydrogen flow (30 ml/min) at a heating rate of 3 °C/min up to 500 ° C and held at this temperature for 2 h . CO<sub>2</sub>, CO, CH<sub>4</sub> and Ar were analyzed online by a SRI 6840 gas chromatography equipped with Carboxene-1000 column and TCD detector, whereas hydrocarbon products were

analyzed online by SRI 6840 gas chromatography with PQ column and FID detector. The selectivity of the products is calculated based on molar flows (mmol/min) as shown in eqs.1-4, and the carbon balance is above 85% in all cases.

$$\text{Conv.}_{\text{CO}_2} = \frac{F_{\text{CO}_2,\text{in}} - F_{\text{CO}_2,\text{out}}}{F_{\text{CO}_2,\text{in}}} \times 100\% \quad \text{eq.1}$$

$$\text{Selec.}_{\text{CO}} = \frac{F_{\text{CO},\text{out}}}{F_{\text{CO}_2,\text{in}} - F_{\text{CO}_2,\text{out}}} \times 100\% \quad \text{eq.2}$$

$$\text{Selec.}_{\text{C}_n\text{H}_m} = \frac{nF_{\text{C}_n\text{H}_m,\text{out}}}{F_{\text{CO}_2,\text{in}} - F_{\text{CO}_2,\text{out}}} \times 100\% \quad \text{eq.3}$$

$$\text{Carbon balance} = \frac{F_{\text{CO},\text{out}} + \sum nF_{\text{C}_n\text{H}_m,\text{out}}}{F_{\text{CO}_2,\text{in}} - F_{\text{CO}_2,\text{out}}} \times 100\% \quad \text{eq.4}$$

### 1.3 Catalyst-bed configuration

The configuration mode is labeled as ‘**Conf. X-n/m**’ where X refers to configuration type involving packed 15Co catalyst along with or without  $\gamma\text{-Al}_2\text{O}_3$  packing (same particle size as 15Co catalyst) as illustrated in **Fig. S2** and ‘n/m’ represents the catalyst-to-alumina packing-height-ratio. Details of each mode in this study are elaborated in **Table S1**.

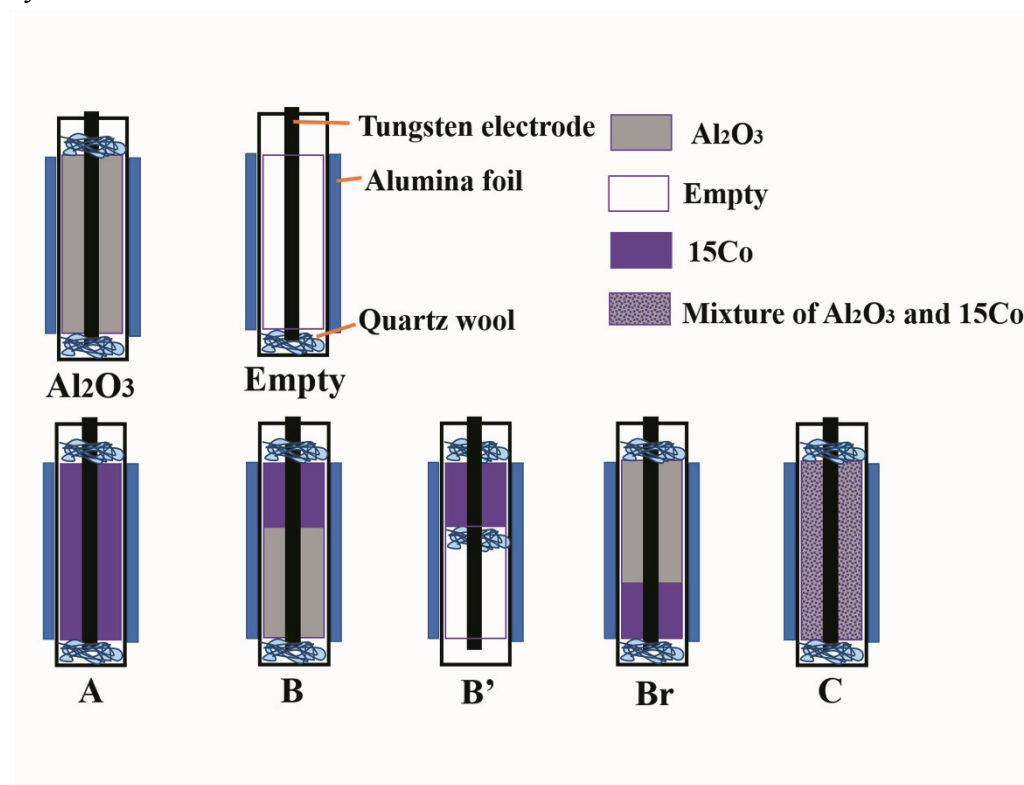


**Fig. S2.** Diagram illustration of the catalyst-bed configuration for plasma-catalytic  $\text{CO}_2$  hydrogenation.

**Table S1.** Details of the catalyst-bed configuration for plasma-catalytic CO<sub>2</sub> hydrogenation reaction.

| Experiments                        | First sector in the bed             |           |           | Second sector in the bed       |          |           |
|------------------------------------|-------------------------------------|-----------|-----------|--------------------------------|----------|-----------|
|                                    | Material                            | Weight/g  | Height/cm | Material                       | Weight/g | Height/cm |
| <b>Al<sub>2</sub>O<sub>3</sub></b> | Al <sub>2</sub> O <sub>3</sub>      | ~1.25     | 5.0       | -                              | 0        | 0         |
| <b>Empty</b>                       | -                                   | -         | 5.0       | -                              | -        | -         |
| <b>Conf. A</b>                     | 15Co                                | 1.25      | 5.0       | -                              | -        | -         |
| <b>Conf. B-1/9</b>                 | 15Co                                | 0.125     | 0.5       | Al <sub>2</sub> O <sub>3</sub> | ~1.125   | 4.5       |
| <b>Conf. B-2/8</b>                 | 15Co                                | 0.25      | 1.0       | Al <sub>2</sub> O <sub>3</sub> | ~1.0     | 4.0       |
| <b>Conf. Br-2/8</b>                | Al <sub>2</sub> O <sub>3</sub>      | ~0.75     | 4.0       | 15Co                           | 0.25     | 1.0       |
| <b>Conf. B-4/6</b>                 | 15Co                                | 0.5       | 2.0       | Al <sub>2</sub> O <sub>3</sub> | ~0.75    | 3.0       |
| <b>Conf. B'-4/6</b>                | 15Co                                | 0.5       | 2.0       | -                              | -        | 3.0       |
| <b>Conf. C (physical mixture)</b>  | 15Co+Al <sub>2</sub> O <sub>3</sub> | 0.5+~0.75 | 5.0       | -                              | -        | -         |

#### 1.4 Reactor temperature for different catalyst-bed configuration at furnace temperature of 250 °C

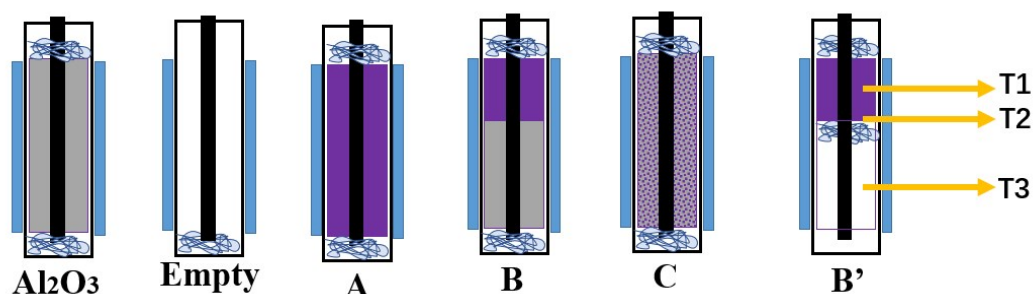


Fig. S3. Position of temperature measuring for different bed configuration.

Table S2. Reactor Temperatures in different Configurations

| Configuration                  | T1/°C | T2/°C | T3/°C |
|--------------------------------|-------|-------|-------|
| Al <sub>2</sub> O <sub>3</sub> | 389   | 398   | 392   |
| Empty                          | 392   | 396   | 393   |
| A                              | 387   | 392   | 387   |
| B                              | 386   | 395   | 391   |
| C                              | 389   | 400   | 394   |
| B'                             | 392   | 402   | 391   |

## 2. Catalyst Characterizations

The porosity properties of the calcined 15Co catalyst and  $\gamma$ -Al<sub>2</sub>O<sub>3</sub> support were measured by Micromeritics TriStar II surface area and porosity analyzer. Surface area, pore volume, and pore diameter were determined from the nitrogen (N<sub>2</sub>) adsorption/desorption isotherms measured at 77 K. All samples were degassed under a N<sub>2</sub> flow at 363 K for 1 h and 473 K for 12 h before analysis. Surface area was calculated according to Brunauer–Emmett–Teller (BET) method, and Barrett–Joyner–Halenda (BJH) model was used to obtain pore volume and average pore diameter.

The temperature-programmed reduction with H<sub>2</sub> (H<sub>2</sub>-TPR) was performed on a Micromeritics Autochem 2920 instrument. The sample (100 mg) was pretreated at 550 °C for 1 h in Ar flow (25 ml/min), then cooled to 50 °C. After that, the sample was exposed to 10% H<sub>2</sub>/Ar mixture (25 ml/min) while heating from 50 to 800 °C at a ramp rate of 10 °C/min to obtain the TPR profile.

In order to characterize the reduced catalyst, it was cooled down under H<sub>2</sub> flow to room temperature after reduction and then passivated with 0.99 vol % O<sub>2</sub>/He (purity > 99.999%) with a flow rate of 30 mL (STP) min<sup>-1</sup> at ambient temperature for overnight in order to preserve the reduced metallic phase after H<sub>2</sub> reduction prior to any further characterization.

The XRD pattern of the reduced catalyst was collected using a PANalytical Empyrean X-ray Diffractometer with Cu K $\alpha$  ( $\lambda = 0.154059$  nm) radiation, fixed slit incidence ( $0.25^\circ$  divergence,  $0.5^\circ$  antiscatter, 10 mm specimen length), and diffracted ( $0.25^\circ$  antiscatter, 0.02 mm nickel filter) optics. Data were collected at 45 kV and 40 mA from  $30$  to  $90^\circ$  ( $2\theta$ ) using a PIXcel detector in scanning mode and 255 active channels for a duration time of 20 min.

**Table S3.** Pore properties of 15Co catalyst and support Al<sub>2</sub>O<sub>3</sub>.

| Sample                         | Surface Area/ m <sup>2</sup> /g | Pore volume/ cm <sup>3</sup> /g | Pore size/ nm |
|--------------------------------|---------------------------------|---------------------------------|---------------|
| Al <sub>2</sub> O <sub>3</sub> | 139                             | 1.04                            | 2.4           |
| 15Co                           | 110.8                           | 0.78                            | 2.4           |

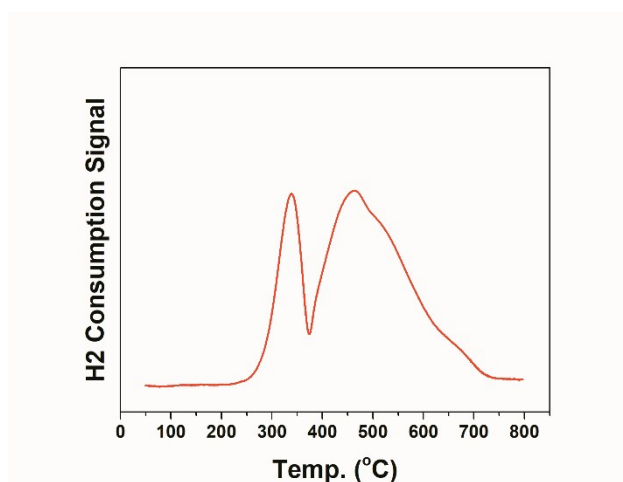


**Fig. S4.** H<sub>2</sub>-TPR profile of the 15Co catalyst.

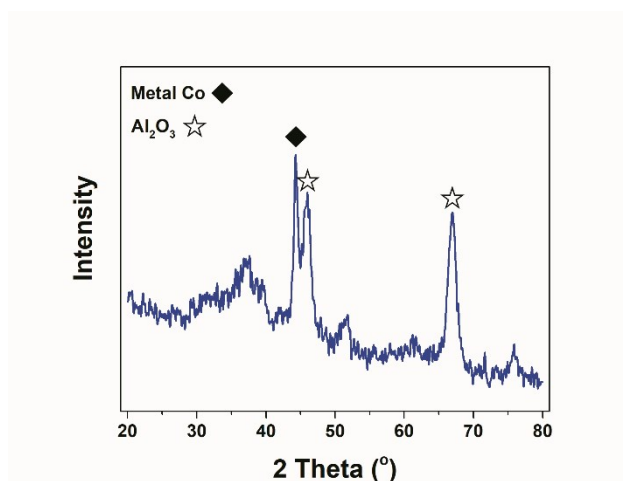


**Fig. S5.** XRD pattern of the reduced 15Co catalyst.

### 3. Results of thermal catalytic reaction over Co catalyst

**Table S4.** Thermal catalytic reactions with different temperature over Conf. B

| Temperature | CO <sub>2</sub> con. | CH <sub>4</sub> Sel. | CO Sel. | C2-C5 Sel. | Carbon Balance |
|-------------|----------------------|----------------------|---------|------------|----------------|
|-------------|----------------------|----------------------|---------|------------|----------------|

| /<br>°C | /% | /%   | /%  | /%  | /%   |
|---------|----|------|-----|-----|------|
| 200     | 10 | 80.6 | 2.8 | 1.6 | 85.0 |
| 250     | 35 | 86.2 | 2.3 | 1.7 | 90.2 |
| 350     | 69 | 87.5 | 2.5 | 1.2 | 90.8 |
| 400     | 71 | 92.0 | 2.7 | 1.4 | 96.1 |

Conditions: P =1 bar; CO<sub>2</sub>/H<sub>2</sub>/Ar molar ratio=4/12/4; Height ratio of Catalyst-to-Alumina ratio is 2/8

#### 4. Lissajous curves for different catalyst-bed configurations

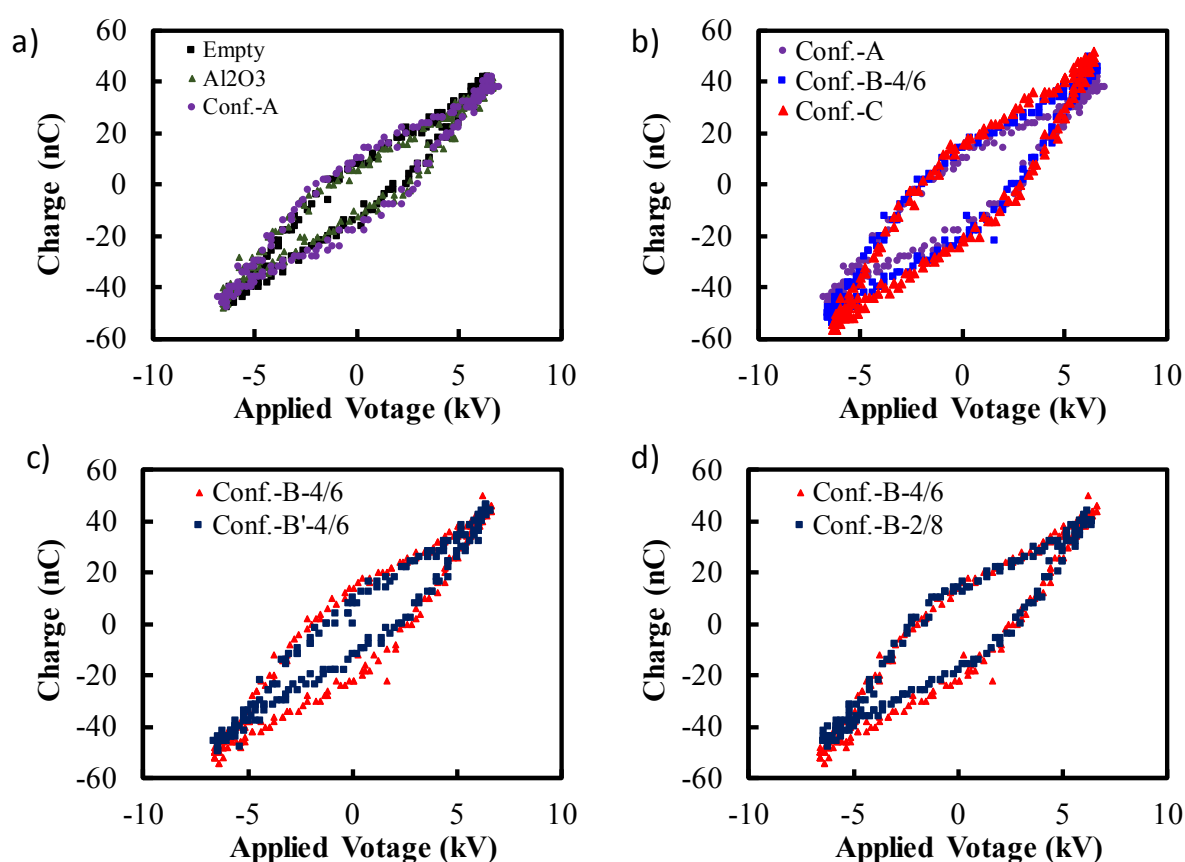


Fig. S6. Lissajous curves of different catalyst-bed configurations.

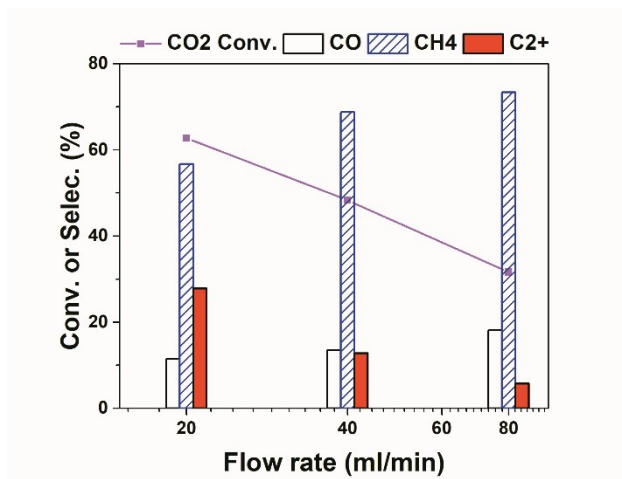
#### 5. Comparison of the performance of Conf. B and Conf. Br.

Table S5. Results of plasma reaction with Conf. B and Conf. Br.

| Configuration type | CO <sub>2</sub> conv. /% | CH <sub>4</sub> Sel. /% | CO Sel. /% | C2-C5 Sel. /% | Carbon Balance /% |
|--------------------|--------------------------|-------------------------|------------|---------------|-------------------|
| Conf. B            | 62.7                     | 56.7                    | 11.4       | 27.8          | 96.0              |
| Conf. Br           | 59.5                     | 82.3                    | 1.5        | 7.5           | 91.1              |

Conditions: Furnace Temperature = 250 °C; P = 1 bar; CO<sub>2</sub>/H<sub>2</sub>/Ar = 4/12/4 ml/min; Voltage = 13.6 kV, Frequency = 23.5 kHz; the Catalyst-to-Alumina packing-height ratio is 2/8.

## 5. Influence of reactant flow rate over Conf. B



**Fig. S7.** Influence of reactant gas flow rate on CO<sub>2</sub> hydrogenation over Conf. B under 4 W of DBD plasma at the furnace temperature of 250 °C. Reaction conditions: 20 v% CO<sub>2</sub> - 60 v% H<sub>2</sub> in Ar balance, H<sub>2</sub>/CO<sub>2</sub> = 3, P= 1 atm, Voltage = 13.6 kV, Frequency = 23.5 kHz.

## 6. Methane plasma conversion

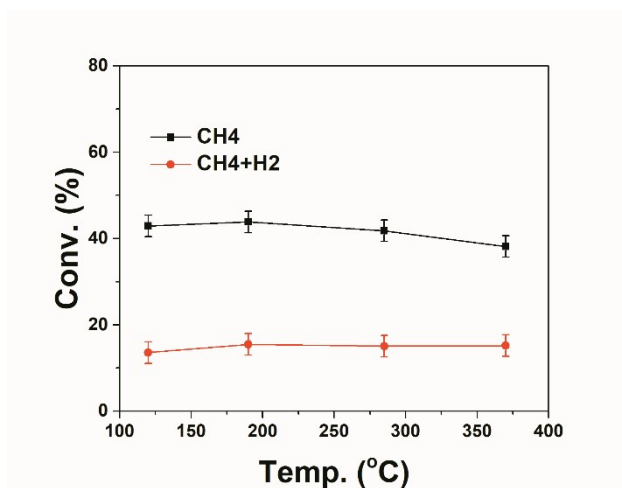


**Fig. S8.** Methane plasma conversion with or without hydrogen. Conditions: Total flow = 20 ml/min, CH<sub>4</sub> flow was fixed at 4 ml/min, H<sub>2</sub> flow was 12 ml/min, and the rest was argon. Pressure = 1 atm, Input voltage = 13.6 kV, Frequency = 23.5 kHz, plasma power = 4 W.

**Table S5.** Products of methane plasma conversion

| Cases                           | Products Molar Distribution/% |      |                 |      |     |                 |     |     |                 |     | O/P <sup>ii</sup> | I/N <sup>iii</sup> |
|---------------------------------|-------------------------------|------|-----------------|------|-----|-----------------|-----|-----|-----------------|-----|-------------------|--------------------|
|                                 | C2 <sup>=</sup>               | C2   | C3 <sup>=</sup> | C3   | iC4 | C4 <sup>=</sup> | nC4 | iC5 | C5 <sup>=</sup> | nC5 |                   |                    |
| CH <sub>4</sub>                 | 14.9                          | 51.0 | 2.2             | 18.7 | 4.2 | 0.9             | 4.3 | 0.8 | 2.4             | 0.7 | 0.25              | 0.98               |
| CH <sub>4</sub> +H <sub>2</sub> | 2.7                           | 73.3 | 0.3             | 15.2 | 2.6 | 0.2             | 2.3 | 1.1 | 1.7             | 0.6 | 0.05              | 1.29               |

i. Conditions: Total flow=20 ml/min, CH<sub>4</sub> flow was fixed at 4 ml/min, H<sub>2</sub> flow was 12 ml/min, and the rest was argon. T=180 °C, Pressure=1 atm, Input voltage=13.6 kV, Frequency=23.5 kHz.

ii. Olefin to paraffin molar ratio (C2–C5);

iii. Iso-paraffin to normal paraffin molar ratio (C4, C5);

## 7. Lissajous figures at different AC voltages applied

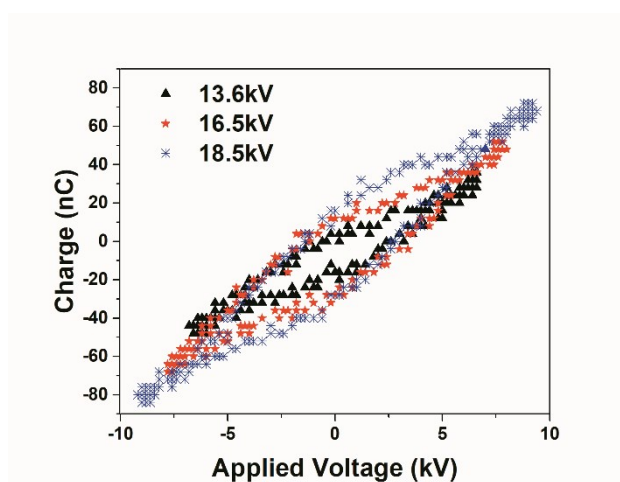


**Fig. S9** Lissajous figures of different voltages on Conf. B-2/8. (Frequency=23.5 kHz)

The calculated plasma power at 13.6 kV, 16.5 kV and 18.8 kV were 3.8 W, 6.9 W and 10.1 W, respectively.

## 8. Comparison in CO<sub>2</sub> hydrogenation performances reported in literature.

**Table S6.** Comparison in CO<sub>2</sub> hydrogenation.

| <b>Catalyst</b>                           | <b>Reaction Type</b> | <b>Operating Temp. (°C)</b> | <b>Pressure (MPa)</b> | <b>CO<sub>2</sub> Con. (%)</b> | <b>CH<sub>4</sub> Sel. (%)</b> | <b>CO Sel. (%)</b> | <b>C<sub>2</sub>+ Sel. (%)</b> | <b>C<sub>2</sub>+ Yield (%)</b> | <b>Ref.</b> |
|---|----------------------|-----------------------------|-----------------------|--------------------------------|--------------------------------|--------------------|--------------------------------|---------------------------------|-------------|
| <b>15% Co/Al<sub>2</sub>O<sub>3</sub></b> | Plasma (4 W)         | 25                          | 0.1                   | 36.0                           | 63.6                           | 16.7               | 5.6                            | 2.0                             | This work   |
| <b>15% Co/Al<sub>2</sub>O<sub>3</sub></b> | Plasma (10 W)        | 25                          | 0.1                   | 76.4                           | 42.6                           | 8.3                | 46.7                           | 35.7                            | This work   |
| <b>Co/ZSM-5</b>                           | Plasma (14 W)        | < 200                       | 0.1                   | 45.0                           | 72.0                           | 14.3               | 13.7                           | 6.2                             | 1           |
| <b>Ni/ZSM-5</b>                           | Plasma (14 W)        | < 200                       | 0.1                   | 46.3                           | 87.9                           | 9.5                | 2.6                            | 1.2                             | 1           |
| <b>Ni/CeZrOx</b>                          | Plasma               | 425                         | 0.1                   | 85                             | 97                             | 2                  | -                              | -                               | 2           |
| <b>10%Ni/zeolite</b>                      | Plasma               | 280+                        | 0.1                   | 90                             | -                              | -                  | -                              | -                               | 3           |
| <b>8%Cu/Al<sub>2</sub>O<sub>3</sub></b>   | Plasma               | -                           | 0.1                   | 23                             | 1.7                            | 96                 | -                              | -                               | 4           |
| <b>FeCu(0.17)</b>                         | Thermal              | 300                         | 1.0                   | 28.5                           | 26                             | 23                 | 51                             | 14.5                            | 5           |
| <b>In<sub>2</sub>O<sub>3</sub>+HZSM-5</b> | Thermal              | 340                         | 3.0                   | 15                             | -                              | 45                 | 50                             | 7.5                             | 6           |
| <b>NiMn/CNT</b>                           | Thermal              | 360                         | 0.1                   | 78                             | 99                             | -                  | -                              | -                               | 7           |

## Reference

1. L. Lan, A. Wang and Y. Wang, *Catalysis Communications*, 2019, **130**, 105761.
2. M. Nizio, A. Albarazi, S. Cavadias, J. Amouroux, M. E. Galvez and P. Da Costa, *International Journal of Hydrogen Energy*, 2016, **41**, 11584-11592.
3. E. Jwa, S. B. Lee, H. W. Lee and Y. S. Mok, *Fuel Processing Technology*, 2013, **108**, 89-93.
4. Y. Zeng and X. Tu, *IEEE Transactions on Plasma Science*, 2016, **44**, 405-411.
5. W. Wang, X. Jiang, X. Wang and C. Song, *Industrial & Engineering Chemistry Research*, 2018, **57**, 4535-4542.
6. P. Gao, S. Li, X. Bu, S. Dang, Z. Liu, H. Wang, L. Zhong, M. Qiu, C. Yang, J. Cai, W. Wei and Y. Sun, *Nat Chem*, 2017, **9**, 1019-1024.
7. J. Li, Y. Zhou, X. Xiao, W. Wang, N. Wang, W. Qian and W. Chu, *ACS Appl Mater Interfaces*, 2018, **10**, 41224-41236.